

# Supplementary Material: Generalized Content-Preserving Warps for Image Stitching

This supplementary document consists of three parts. The first part presents the datasets that we use in our experiments. The second part describes the detailed generation process of synthetic images with different degrees of colour variation, which is related to the Section 3.1 of the paper. The third part provides more comparative results with higher image resolution.

## 1 Datasets



Figure 1: Dataset1 consists of 12 pairs of images. First row: pair 01-06. Second row: pair 07-12. Each pair of images has nearly no colour differences, which are collected from [1, 2, 4]. Dataset1 is used in our synthetic experiments (Section 3.1 of the paper).

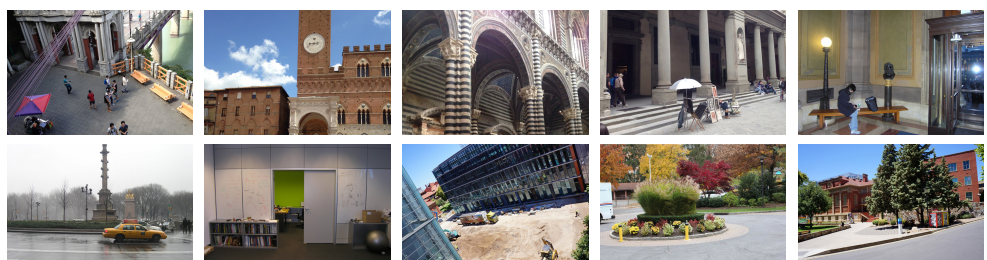


Figure 2: Dataset2 consists of 10 pairs of images. First row: pair 01-05. Second row: pair 06-10. Each pair of images has significant colour differences and are directly collected from [1, 2, 4]. We use Dataset2 to conduct our experiments on real images (Section 3.2 of the paper).

## 2 Generating Images with Colour Variation

As described in the paper, for each pair of images in the Dataset1, we generate  $N$  pairs of images ( $N = 16$  in our implementation) with different degrees of colour variations to obtain

our synthetic data. In order to control the degree of colour variation, we adopt the global colour model [3]:

$$I' = (cI)^\gamma, \quad (1)$$

where  $I$  is the original image,  $I'$  is the synthetic image,  $c$  is a scale factor that is related to the white balance ( $c = 1.0$  in our implementation) and  $(.)^\gamma$  is the non-linear gamma function. In order to create more complex variation that is relevant to spatial positions, we add a spatially-varying factor to the non-linear gamma function and compute the  $\gamma$  of Eq.1 as follows:

$$\gamma = \left(1 + \frac{k-1}{N}\right)^{-a/b} \times \beta, \quad (2)$$

where  $k = 1, 2, 3, \dots, N$  denotes the pair index,  $a$  is the pixel column coordinate (or row coordinate),  $b$  is the image width (or image height). With Eq. 2, we use different values of  $\gamma$  for pixels located on different positions to simulate the local colour variation. We synthesis the colour difference from small to large ( $k$  varies from 1 to  $N$ ) according to the colour model defined by Eq. 1. Specifically, we first convert the source image from  $RGB$  colour space to  $YCbCr$  colour space. We then conduct colour transformation for each image channel independently. For image  $Y$ -channel, we sample the value of  $\beta$  from 1.0 to 0.5. For other two image channels, we sample  $\beta$  from 1.0 to 0.95. Figure 3 presents one group of our synthetic images.

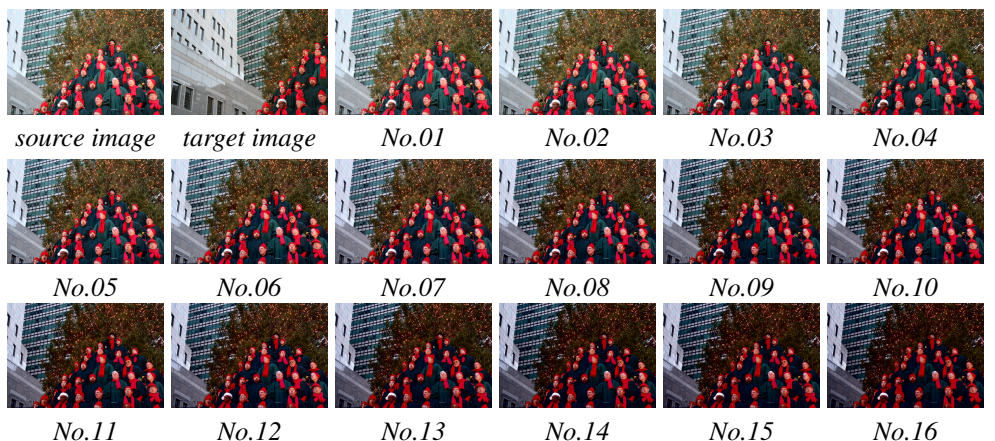


Figure 3: One group of synthetic images generated with our scheme. It consists of 16 pairs of images. We control the colour differences from small to large.

### 3 Comparative Results

In this part, we present more comparative results with higher image resolution. Specifically, Figure 4 to Figure 9 shows our results on all 12 groups of synthetic images of Dataset1. As for experiments on Dataset2, from Figure 10 to Figure 13, we present the results of our method compared with Global Homography, CPW and DF-W. From Figure 14 to Figure 19, we present the detailed results of our method compared with DF-W, MF-W, LSH+MF-W and ROS+MF-W.

## 092 References

- 093
- 094 [1] Yu-Sheng Chen and Yung-Yu Chuang. Natural image stitching with the global similarity  
095 prior. In *European Conference on Computer Vision (ECCV)*, pages 186–201, 2016.
- 096 [2] Shiwei Li, Lu Yuan, Jian Sun, and Long Quan. Dual-feature warping-based motion  
097 model estimation. In *IEEE International Conference on Computer Vision (ICCV)*, pages  
098 4283–4291, 2015.
- 099
- 100 [3] Jaesik Park, Yu-Wing Tai, Sudipta N Sinha, and In So Kweon. Efficient and robust color  
101 consistency for community photo collections. In *IEEE Conference on Computer Vision  
102 and Pattern Recognition (CVPR)*, pages 430–438, 2016.
- 103 [4] Julio Zaragoza, Tat-Jun Chin, Michael S Brown, and David Suter. As-projective-as-  
104 possible image stitching with moving dlt. In *IEEE Conference on Computer Vision and  
105 Pattern Recognition (CVPR)*, pages 2339–2346, 2013.
- 106
- 107
- 108
- 109
- 110
- 111
- 112
- 113
- 114
- 115
- 116
- 117
- 118
- 119
- 120
- 121
- 122
- 123
- 124
- 125
- 126
- 127
- 128
- 129
- 130
- 131
- 132
- 133
- 134
- 135
- 136
- 137

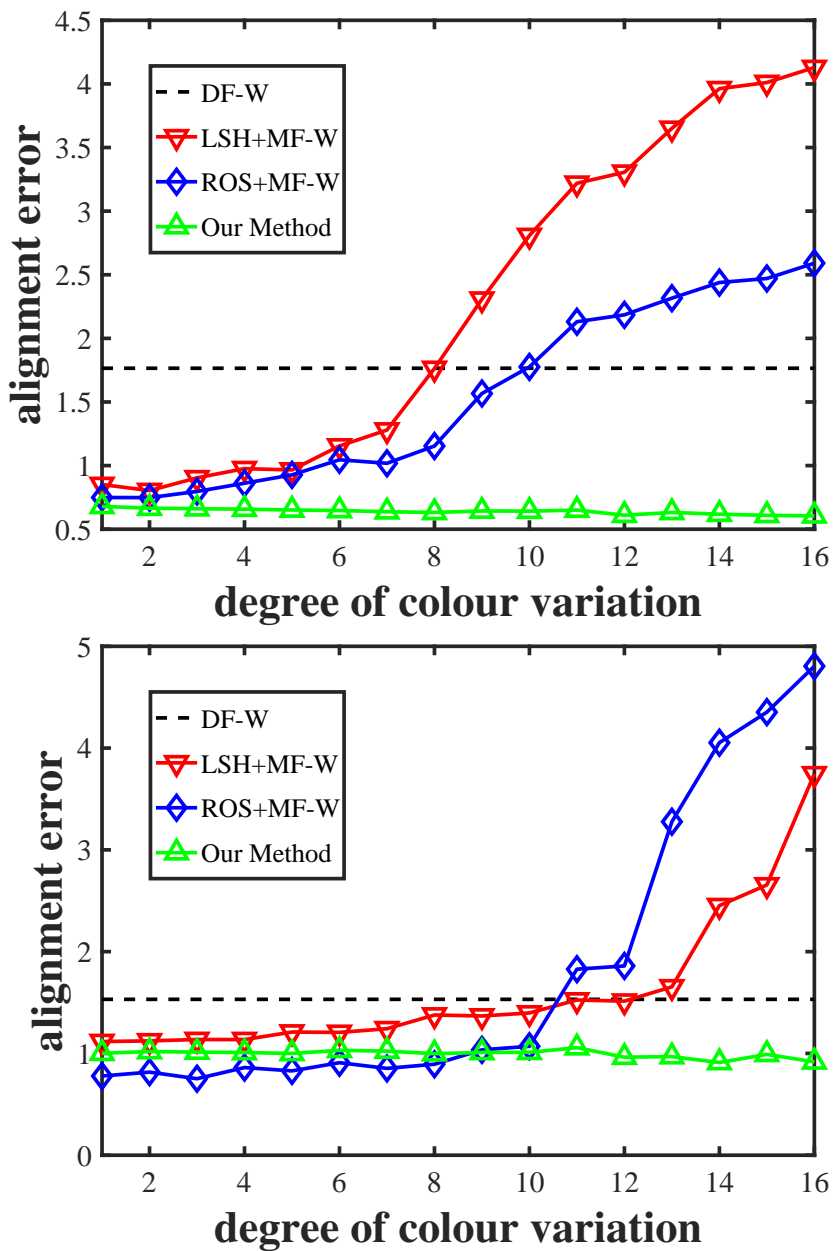


Figure 4: Comparative results on image pair 01-02.

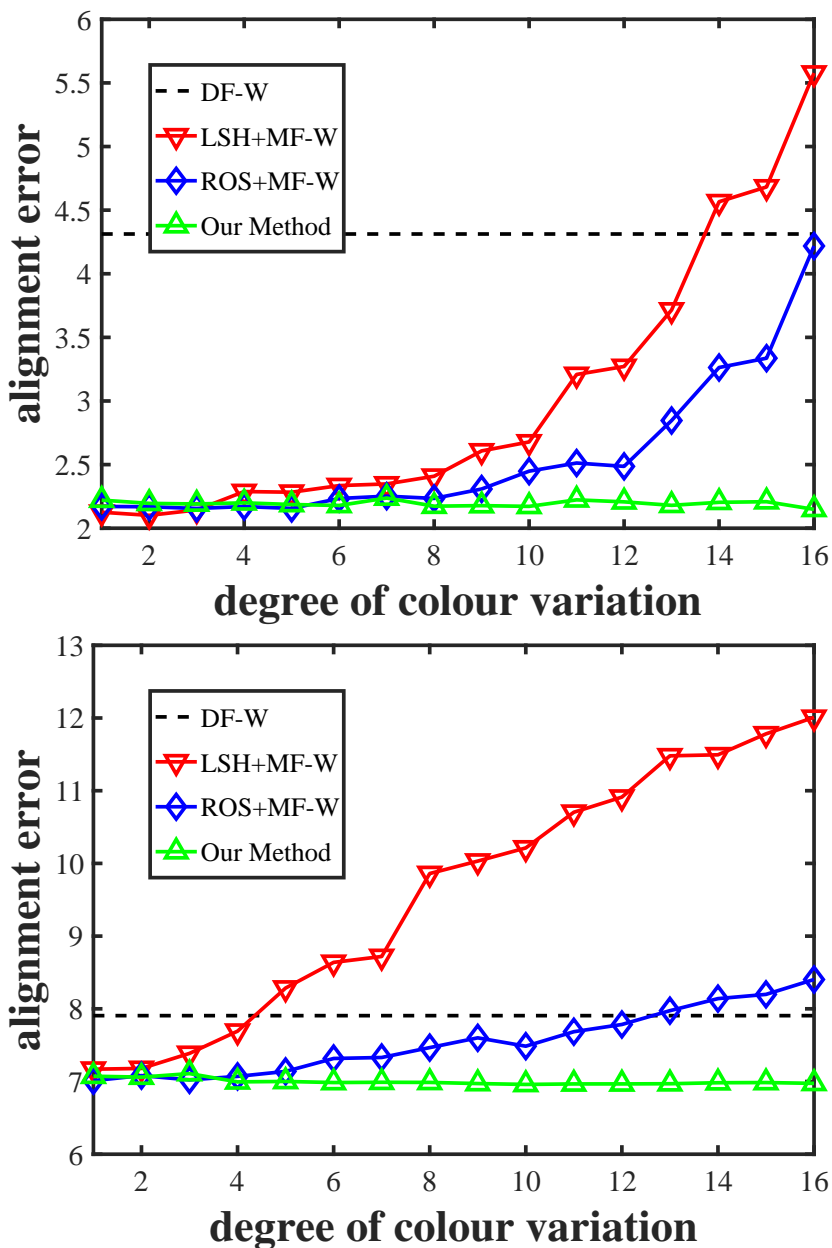


Figure 5: Comparative results on image pair 03-04.

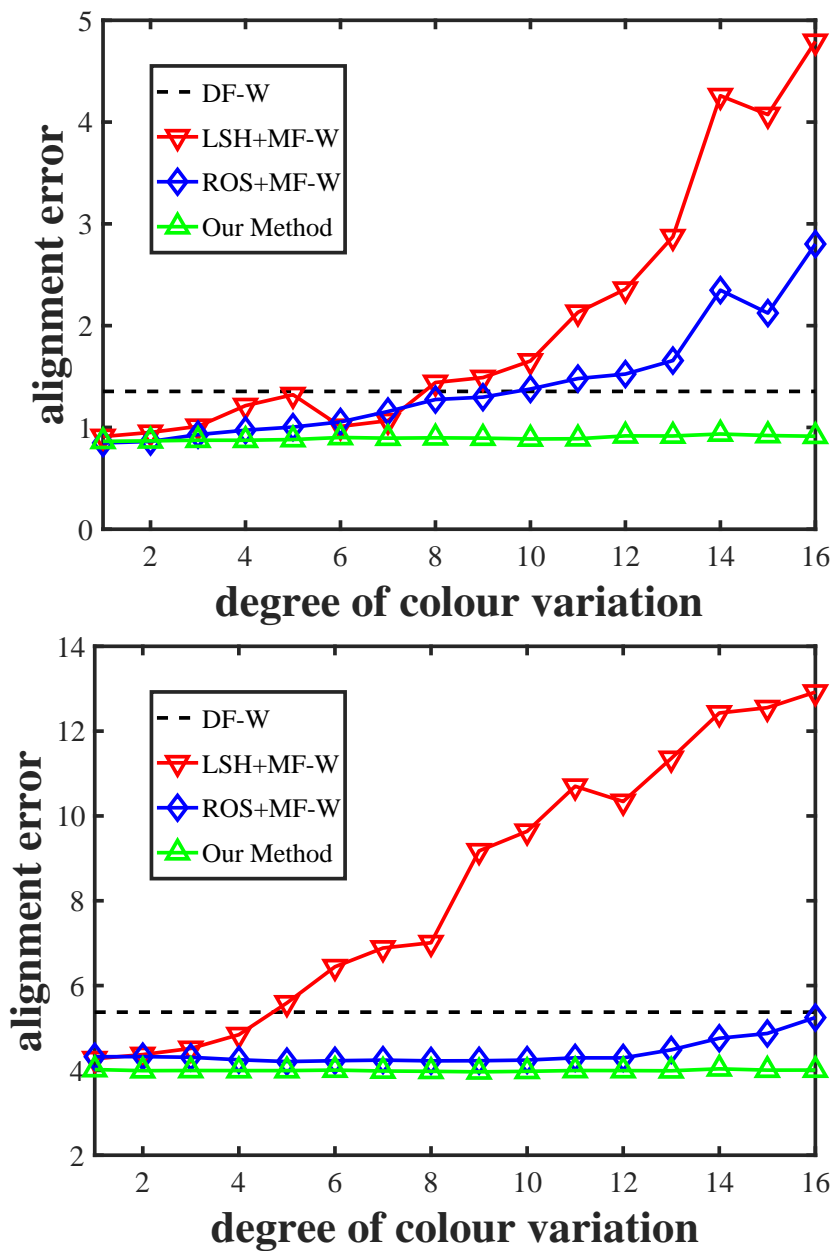


Figure 6: Comparative results on image pair 05-06.

230  
231  
232  
233  
234  
235  
236  
237  
238  
239  
240  
241  
242  
243  
244  
245  
246  
247  
248  
249  
250  
251  
252  
253  
254  
255  
256  
257  
258  
259  
260  
261  
262  
263  
264  
265  
266  
267  
268  
269  
270  
271  
272  
273  
274  
275

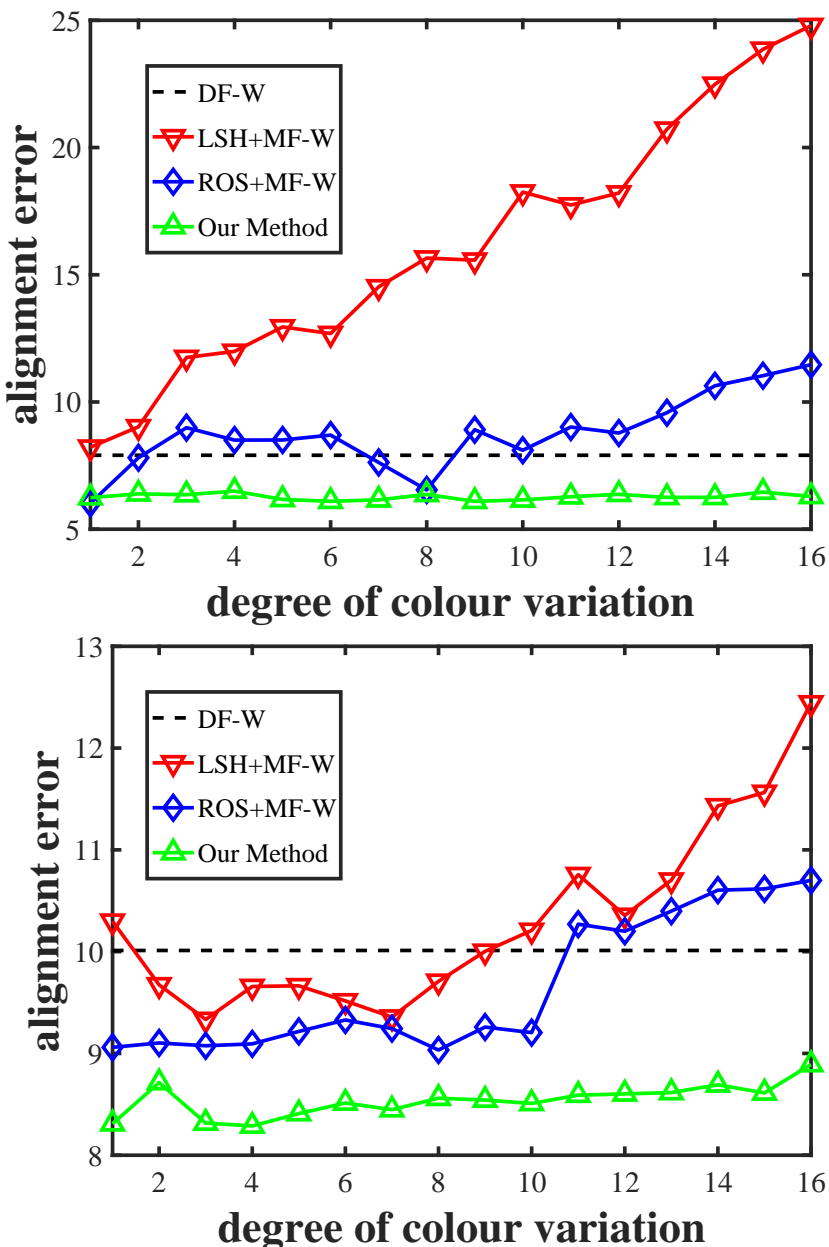


Figure 7: Comparative results on image pair 07-08.

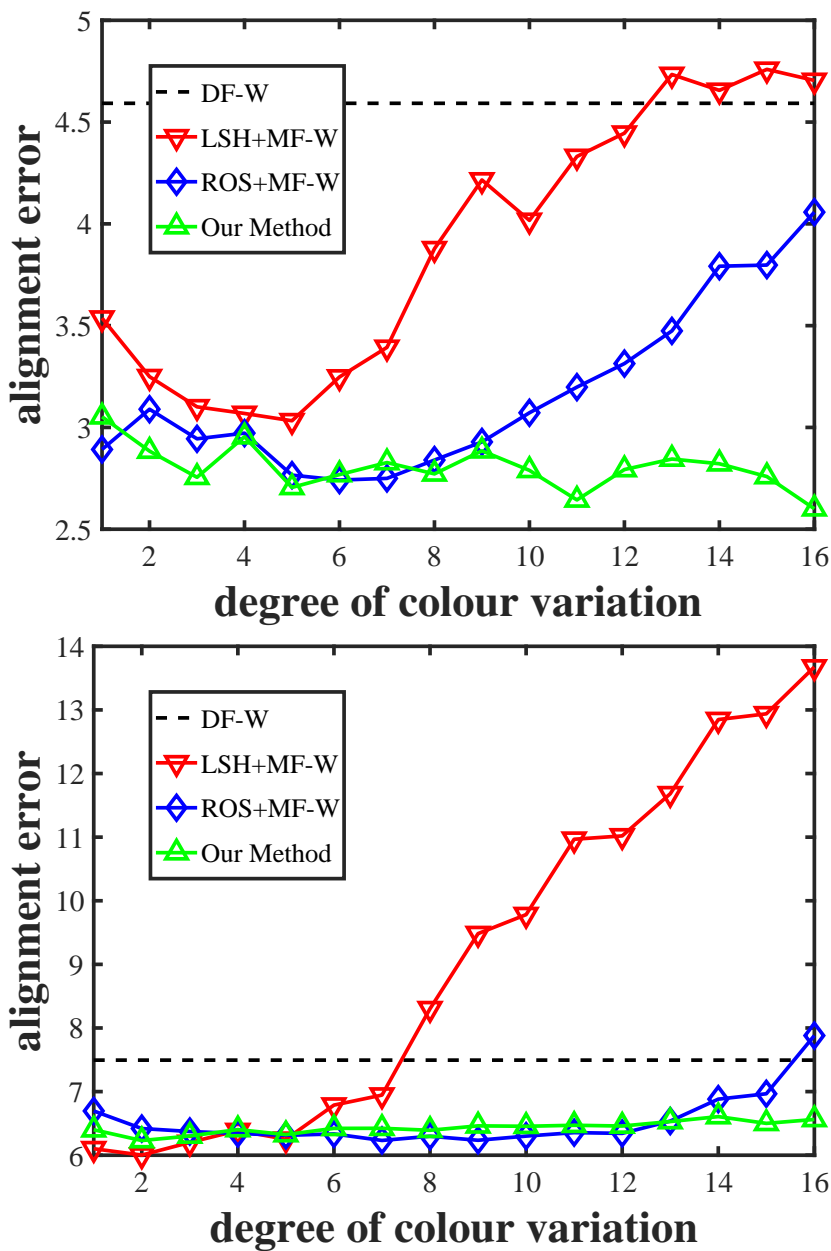


Figure 8: Comparative results on image pair 09-10.

322  
323  
324  
325  
326  
327  
328  
329  
330  
331  
332  
333  
334  
335  
336  
337  
338  
339  
340  
341  
342  
343  
344  
345  
346  
347  
348  
349  
350  
351  
352  
353  
354  
355  
356  
357  
358  
359  
360  
361  
362  
363  
364  
365  
366  
367

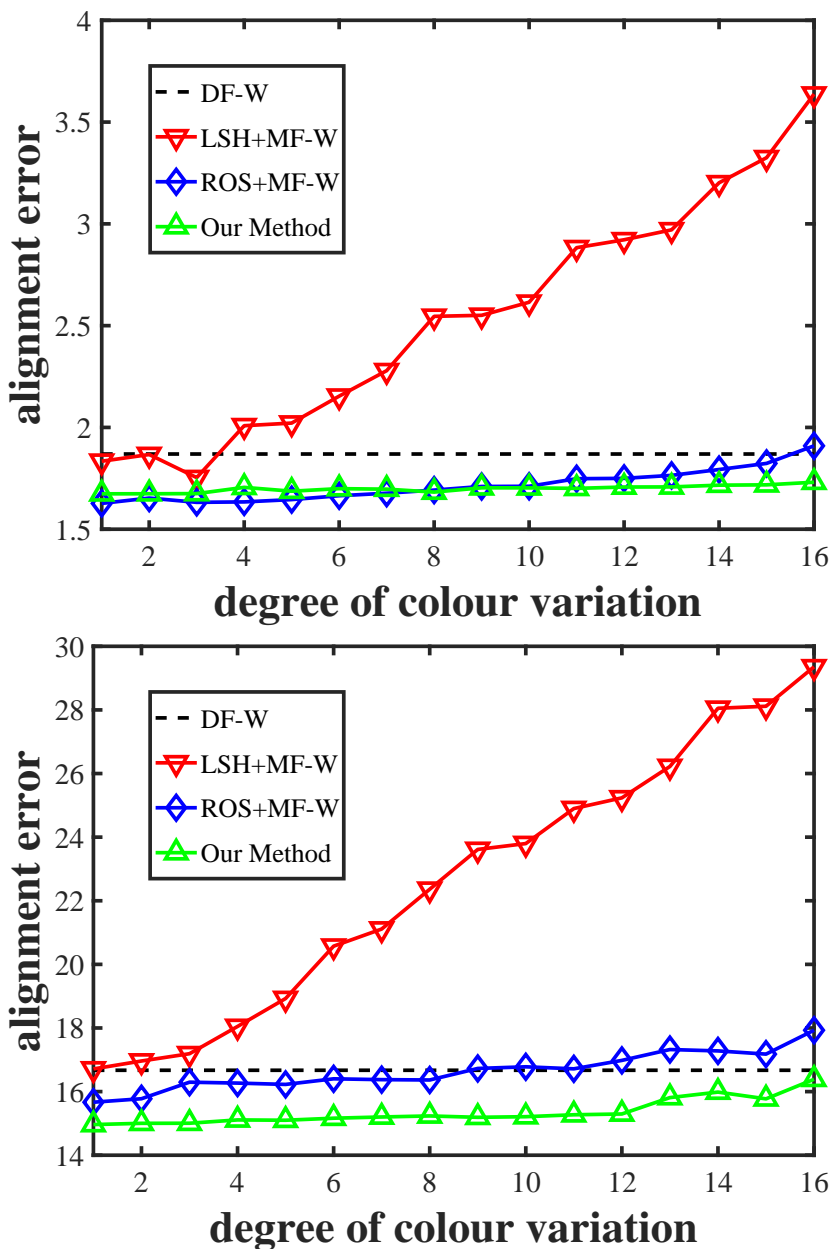
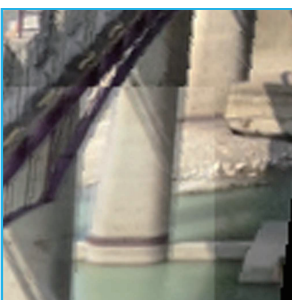
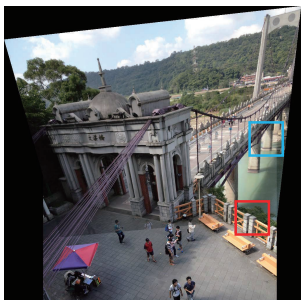
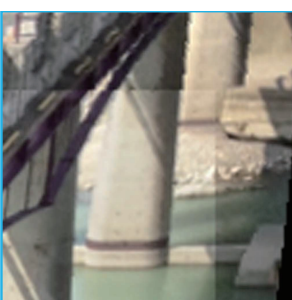
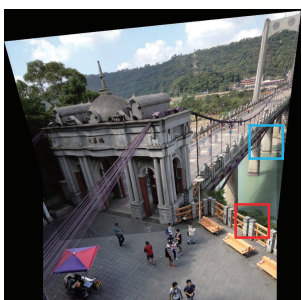


Figure 9: Comparative results on image pair 11-12.

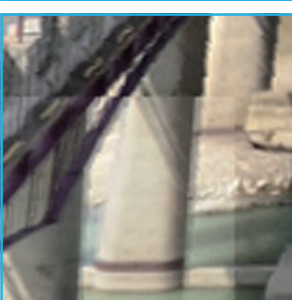
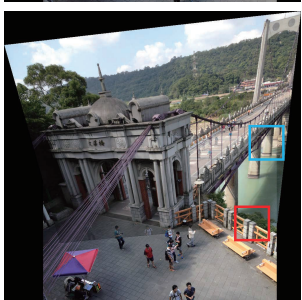
Global



CPW



DF-W



Ours

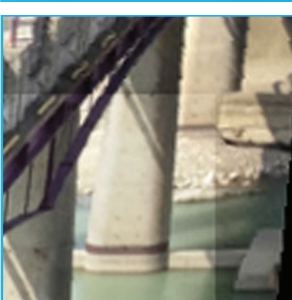
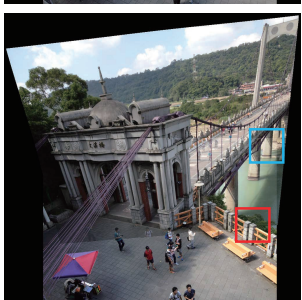


Figure 10: Comparisons with Global Homography, CPW and DF-W: Image pair 01.

414

415

416

417

418

419

420

421

422

423

424

425

426

427

428

429

430

431

432

433

434

435

436

437

438

439

440

441

442

443

444

445

446

447

448

449

450

451

452

453

454

455

456

457

458

459

460  
461  
462  
463  
464  
465  
466  
467  
468  
469  
470  
471  
472  
473  
474  
475  
476  
477  
478  
479  
480  
481  
482  
483  
484  
485  
486  
487  
488  
489  
490  
491  
492  
493  
494  
495  
496  
497  
498  
499  
500  
501  
502  
503  
504  
505

Global  
CPW  
DF-W  
Ours

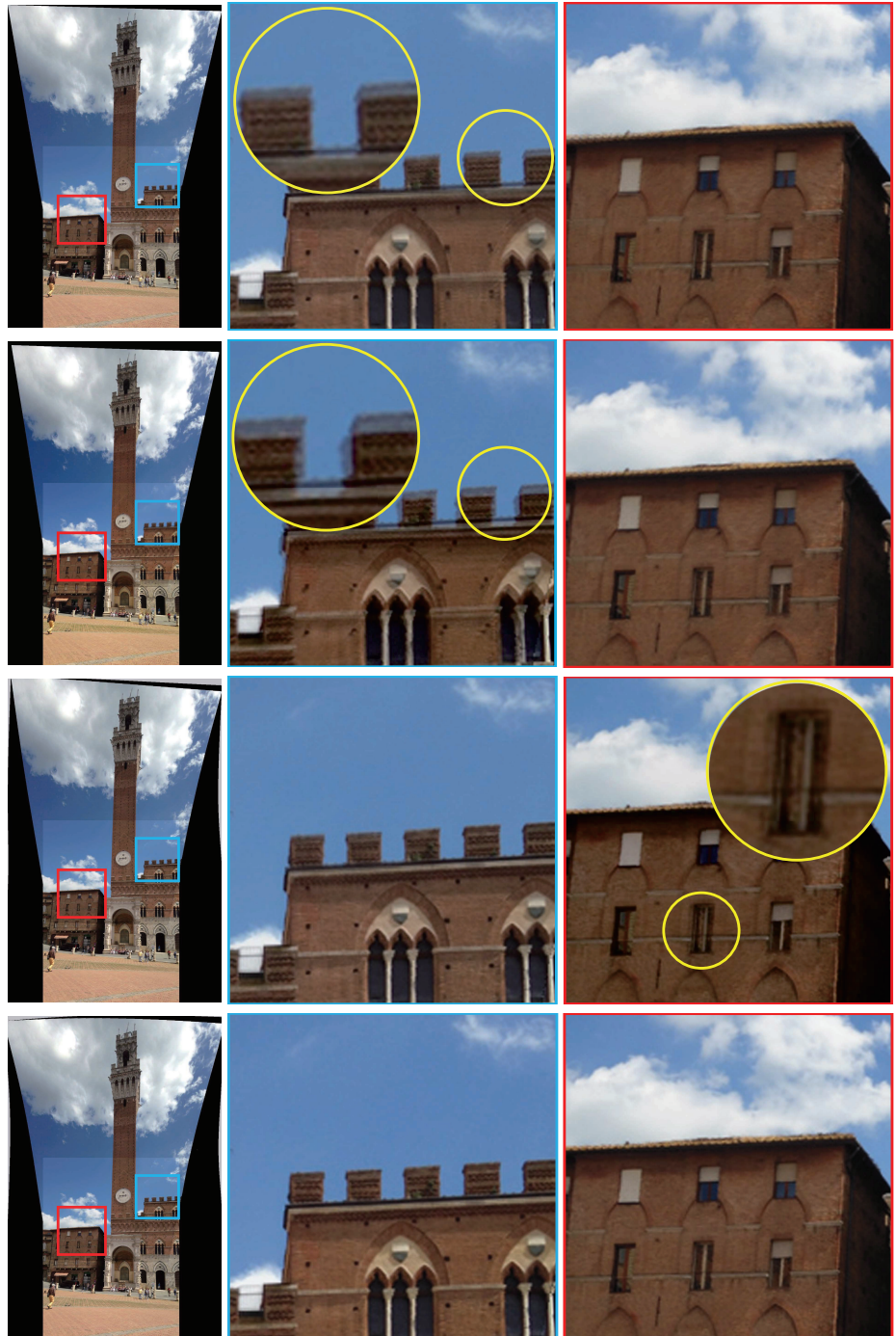
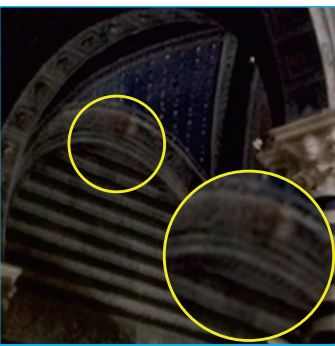
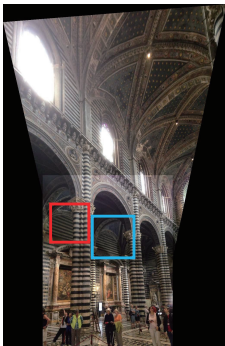
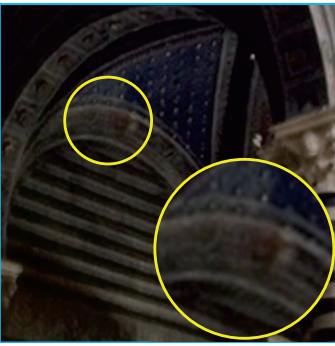
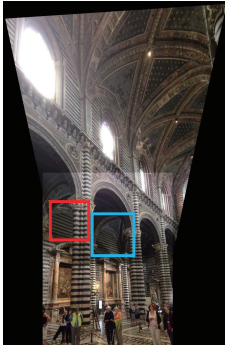


Figure 11: Comparisons with Global Homography, CPW and DF-W: Image pair 02.

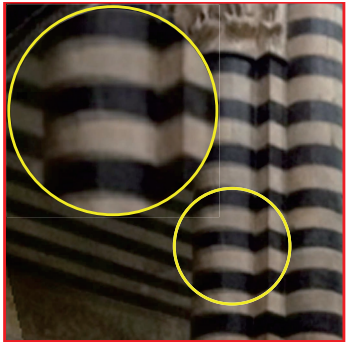
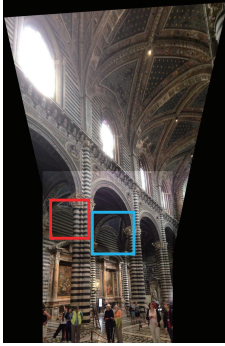
Global



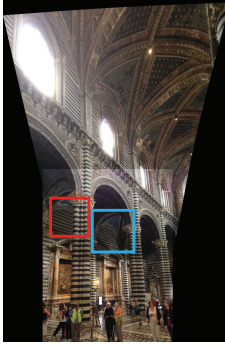
CPW



DF-W



Ours



506  
507  
508  
509  
510  
511  
512  
513  
514  
515  
516  
517  
518  
519  
520  
521  
522  
523  
524  
525  
526  
527  
528  
529  
530  
531  
532  
533  
534  
535  
536  
537  
538  
539  
540  
541  
542  
543  
544  
545  
546  
547  
548  
549  
550  
551

Figure 12: Comparisons with Global Homography, CPW and DF-W: Image pair 03.

552

553

554

555

556

557

558

559

560

561

562

563

564

565

566

567

568

569

570

571

572

573

574

575

576

577

578

579

580

581

582

583

584

585

586

587

588

589

590

591

592

593

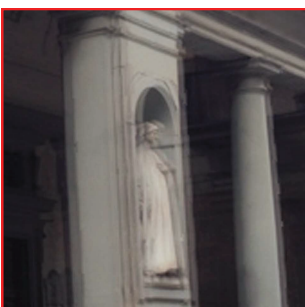
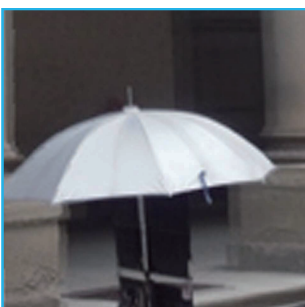
594

595

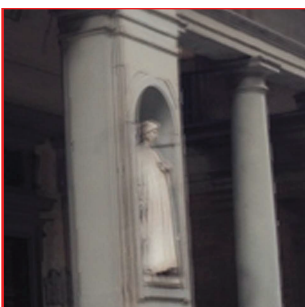
596

597

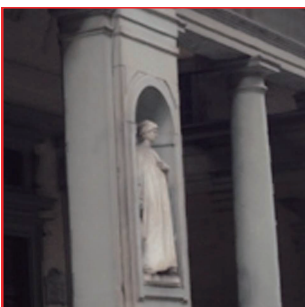
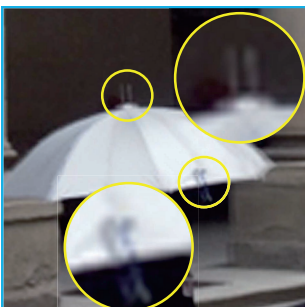
Global



CPW



DF-W



Ours

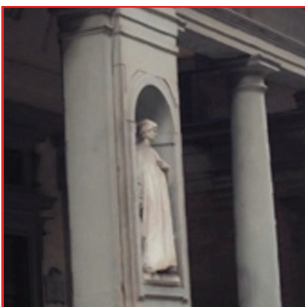
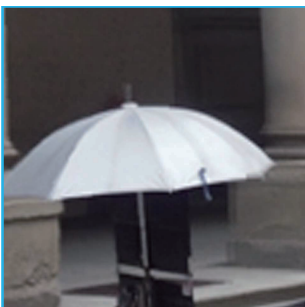
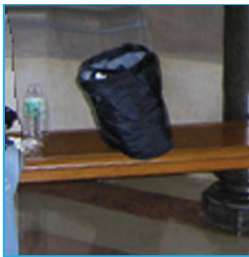


Figure 13: Comparisons with Global Homography, CPW and DF-W: Image pair 04.

DF-W



MF-W



LSH+MF-W



ROS+MF-W



Ours

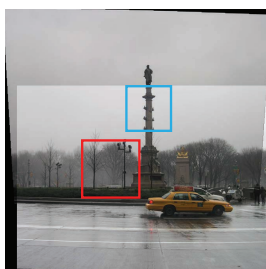


Figure 14: Comparisons with DF-W, MF-W, LSH+MF-W and ROS+MF-W: Image pair 05.

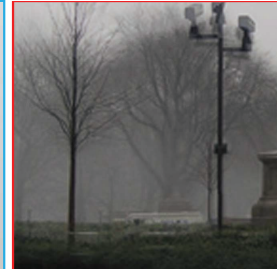
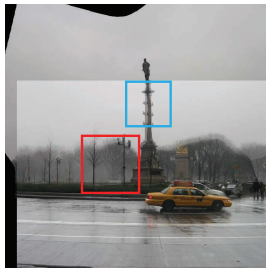
598  
599  
600  
601  
602  
603  
604  
605  
606  
607  
608  
609  
610  
611  
612  
613  
614  
615  
616  
617  
618  
619  
620  
621  
622  
623  
624  
625  
626  
627  
628  
629  
630  
631  
632  
633  
634  
635  
636  
637  
638  
639  
640  
641  
642  
643

644  
645  
646  
647  
648  
649  
650  
651  
652

DF-W

653  
654  
655  
656  
657  
658  
659  
660  
661

MF-W

662  
663  
664  
665  
666  
667  
668  
669

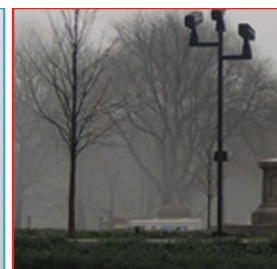
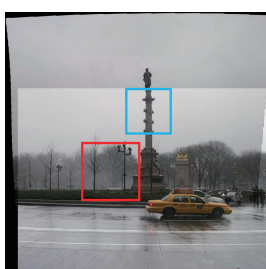
LSH+MF-W

670  
671  
672  
673  
674  
675  
676  
677  
678

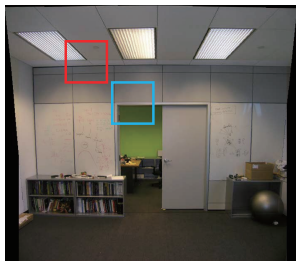
ROS+MF-W

679  
680  
681  
682  
683  
684  
685  
686

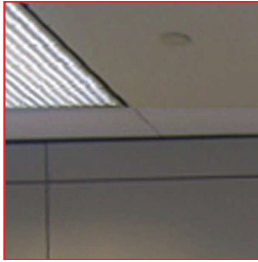
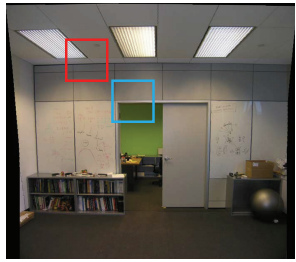
Ours

687 Figure 15: Comparisons with DF-W, MF-W, LSH+MF-W and ROS+MF-W:  
688 Image pair 06.  
689

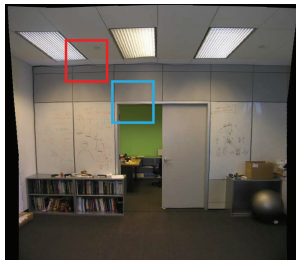
DF-W



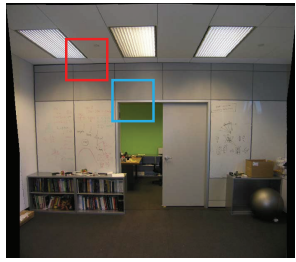
MF-W



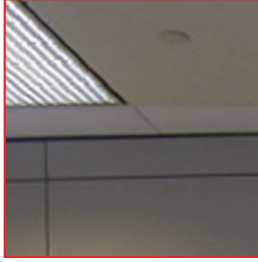
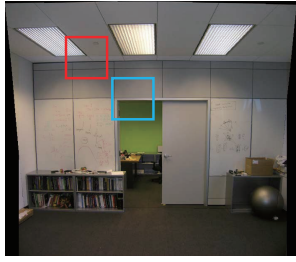
LSH+MF-W



ROS+MF-W



Ours



690  
691  
692  
693  
694  
695  
696  
697  
698  
699  
700  
701  
702  
703  
704  
705  
706  
707  
708  
709  
710  
711  
712  
713  
714  
715  
716  
717  
718  
719  
720  
721  
722  
723  
724  
725  
726  
727  
728  
729  
730  
731  
732  
733  
734  
735

Figure 16: Comparisons with DF-W, MF-W, LSH+MF-W and ROS+MF-W:  
Image pair 07.

736

737

738

739

740

741

742

743

744

745

746

747

748

749

750

751

752

753

754

755

756

757

758

759

760

761

762

763

764

765

766

767

768

769

770

771

772

773

774

775

776

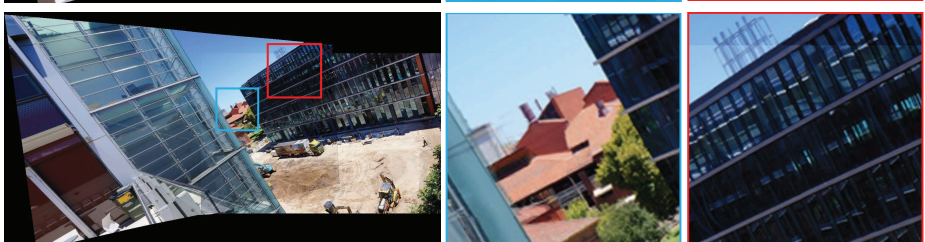
DF-W



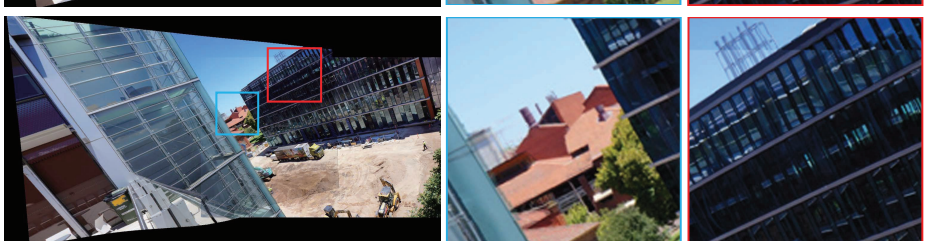
MF-W



LSH+MF-W



ROS+MF-W



Ours

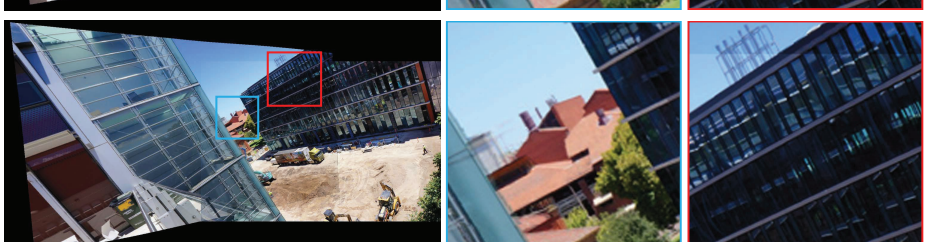


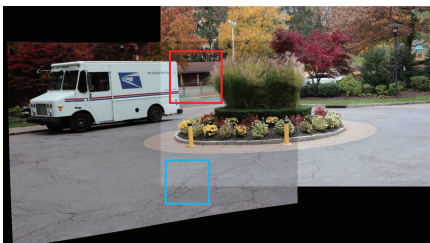
Figure 17: Comparisons with DF-W, MF-W, LSH+MF-W and ROS+MF-W: Image pair 08.

779

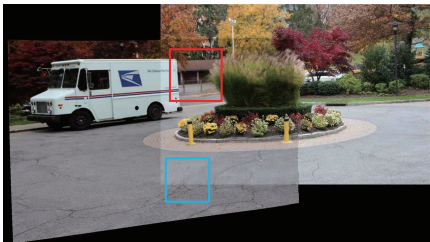
780

781

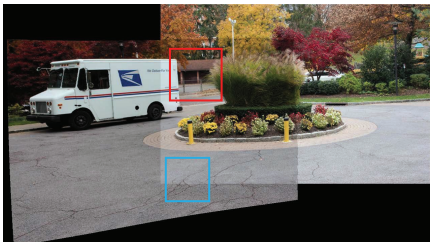
DF-W



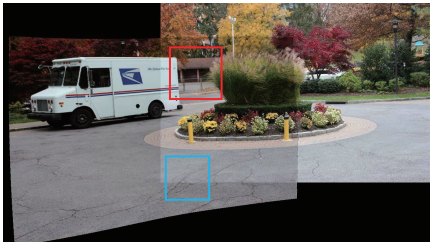
MF-W



LSH+MF-W



ROS+MF-W



Ours

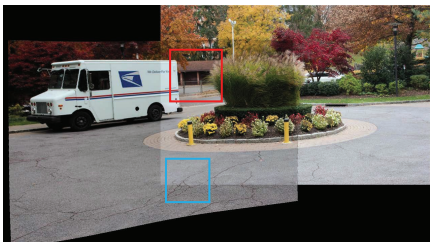


Figure 18: Comparisons with DF-W, MF-W, LSH+MF-W and ROS+MF-W: Image pair 09.

782

783

784

785

786

787

788

789

790

791

792

793

794

795

796

797

798

799

800

801

802

803

804

805

806

807

808

809

810

811

812

813

814

815

816

817

818

819

820

821

822

823

824

825

826

827

828

829

830

831

832

833

834

835

836

837

838

839

840

841

842

843

844

845

846

847

848

849

850

851

852

853

854

855

856

857

858

859

860

861

862

863

864

865

866

867

868

869

870

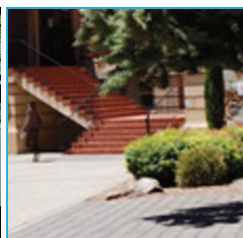
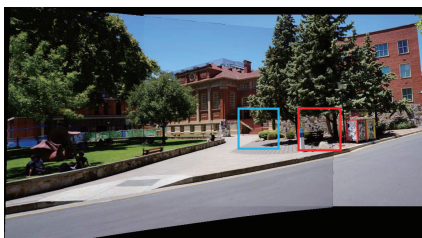
10.

871

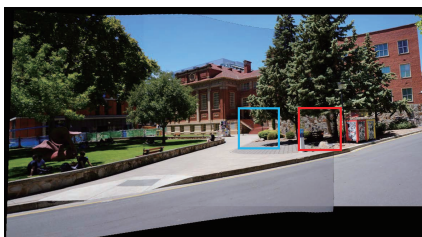
872

873

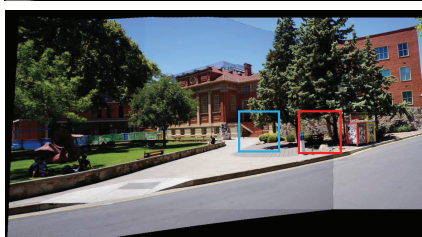
DF-W



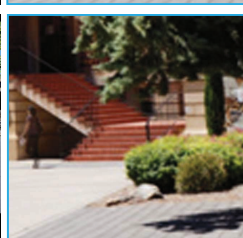
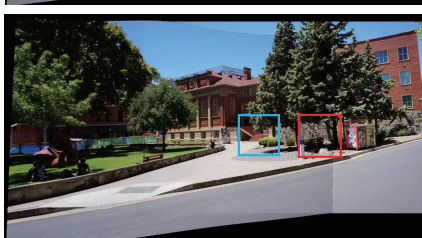
MF-W



LSH+MF-W



ROS+MF-W



Ours

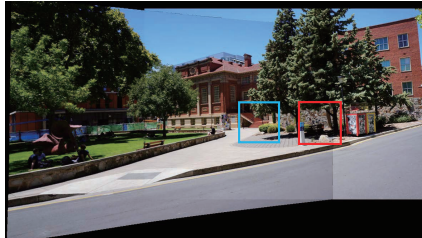


Figure 19: Comparisons with DF-W, MF-W, LSH+MF-W and ROS+MF-W: Image pair 10.